

Rydberg States and Ionization Potential of Calcium Monofluoride

J. E. Murphy, J. M. Berg,^(a) A. J. Merer,^(b) Nicole A. Harris, and R. W. Field

Department of Chemistry, Massachusetts Institute of Technology, Cambridge, Massachusetts 02139

(Received 23 April 1990)

61 vibronic states of CaF in the region 41930–45905 cm⁻¹ are observed by optical-optical double resonance, rovibronically assigned, and shown to belong to 37 Rydberg electronic states. These states are organized into six core-penetrating ($l \leq 2$), mixed- l Rydberg series, from which we obtain an improved value of the CaF ionization potential, 47005 ± 20 cm⁻¹. All previously observed low Rydberg and valence states of CaF fit smoothly into these six Rydberg series, which form the *complete* set of $l \leq 2$ series. Using this information, absolute quantum defects have been determined and the series are assigned *nominally* (i.e., dominant l character) as d (Δ , Π , and Σ), p (Π and Σ), and s (Σ).

PACS numbers: 33.80.Rv, 33.10.Jz, 33.20.Lg, 33.40.Ta

This Letter reports new electronic spectra of CaF in which the *complete* manifold of core-penetrating Rydberg states with orbital angular momentum $l \leq 2$ has been identified, for values of the effective principal quantum number n^* between 4 and 10. The work is significant because CaF is far more ionic than any other diatomic molecule for which similar data exist. The fact that the CaF⁺ ion core is doubly closed shell (Ca²⁺ $1S$, F⁻ $1S$) means that the spectrum and its interpretation will be greatly simplified. The large dipole moment of the CaF⁺ ion core causes significant mixing of states with l differing by 1, particularly at low l values where the Rydberg electron can penetrate deeply into the core. The completeness of the data, including *all* of the core-penetrating Rydberg series, is unique and will permit a very thorough analysis of the interaction between the Rydberg electron and the CaF⁺ ion at short range. The observed Rydberg series are found to extrapolate smoothly back to include *all* the lower-energy electronic states known from previous work. The lowest-energy electronic states (valence states) are well represented by a ligand-field model where a nonbonding electron centered on Ca²⁺ is perturbed by a negative point charge (the ligand).¹ The structure of the inner loops of core-penetrating Rydberg orbitals will resemble the structure of their "valence"-state precursor orbitals and will also be centered on Ca²⁺.² CaF is an example of a new type of Rydberg molecule, one whose stable electronic states are all Rydberg states, in particular including the ground state which is neither repulsive nor weakly bound.³ CaF, as one of the simplest alkaline-earth monohalides, is the prototype for a number of interesting alkaline-earth-containing systems,⁴ where it will be instructive to examine quantitatively the variations of their electronic properties.

There have been several recent studies of high- l Rydberg states in diatomic molecules.⁵⁻⁸ For example, the Rydberg spectrum of NO has been studied extensively and several nl Rydberg series have been identified.^{5,9} The Rydberg states of NO, like CaF, are built on a $1\Sigma^+$ ion core, but for NO the dipole moment of the ion core is so small that no core-dipole-induced l -mixing effects have been detected. Using a long-range force model, the

quadrupole moment and the polarizability of the NO⁺ ion core have been deduced from the term energies of the nonpenetrating nf series.⁵ Using a similar approach, but including the long-range effects of a core dipole, we hope eventually to observe and deperturb the core-nonpenetrating ($l > 2$) Rydberg states of CaF in order to determine the dipole and higher multiple moments and the polarizability of the CaF⁺ ion core. It may also prove possible to extract similar information from core-penetrating s , p , and d series by incorporating a ligand-field model for core-penetration effects into a long-range force model.

Calcium monofluoride is produced in a Broida-type oven modified for high-temperature operation. Crystalline CaF₂ and a small amount of boron (powder or chips) are placed in a graphite crucible, which is resistively heated in a tungsten basket. CaF molecules are entrained in flowing argon carrier gas at a typical pressure of about 200 mTorr. Rydberg states are detected using a pulsed optical-optical double-resonance (OODR) scheme. In the first step (pump), CaF is excited from the ground state $X^2\Sigma^+$ to the $A^2\Pi_{3/2}$ state, using a pulse-amplified ring dye laser tuned to a specific $A-X$ rotational line. In the second step (probe), a frequency-doubled pulsed dye laser excites the molecules to the various Rydberg levels. The spectrum is recorded by detecting uv fluorescence while the probe laser frequency is scanned. The $A^2\Pi_{3/2}$ $v=0$, $J''=3.5$ (e parity) level is the intermediate state in all of the survey scans.

Most of the observed Rydberg states are near the Hund's-case "b" coupling limit, with only the lowest-energy $^2\Pi$ and $^2\Delta$ states having resolvable spin-orbit splittings. When the spin-orbit constant is less than 1 cm⁻¹, $^2\Pi$ and $^2\Delta$ Rydberg states typically appear in the OODR spectrum as a four-line pattern, (O -, P -, Q -, R -form branches) consisting of one line from each of the six rotational branches, but where the PQ and P lines and the QR and Q lines are unresolved. Some representative spectra are shown in Fig. 1. For $^2\Sigma^+$ states, a two-line pattern (P - and R -form branches) is observed via $J''+3.5$ because the spin-rotation splitting is not resolved at such low J . It is possible to distinguish $^2\Delta$ states from $^2\Pi$ states by pumping the $J''=1.5$ ($N''=2$)

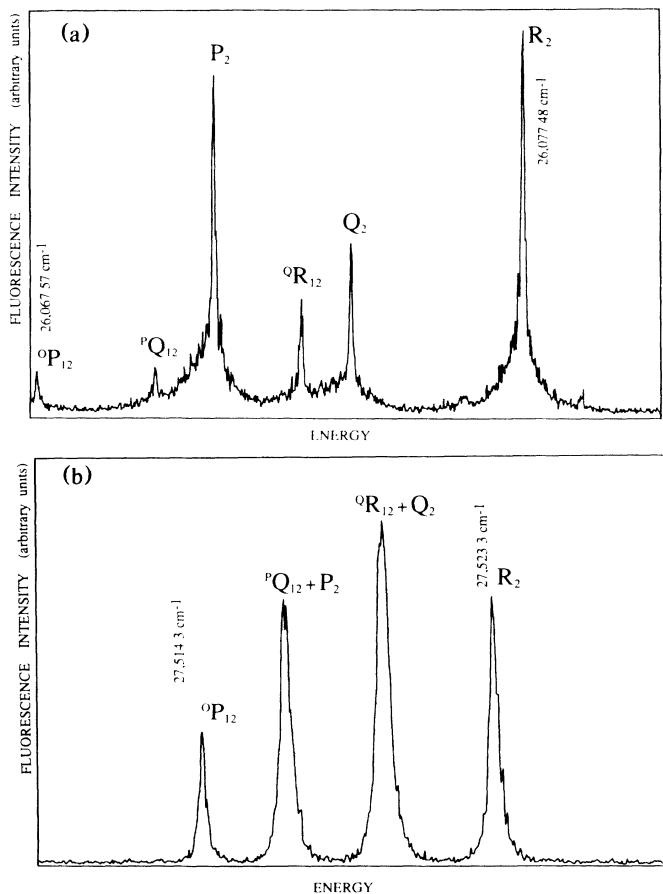


FIG. 1. Representative OODR spectra showing near case-"b" coupling. (a) The $5d \Pi$, $v=2$ ($n^*=4.38$, 42648 cm^{-1})- $A^2\Pi_{3/2}$, $v''=0$, $J''=0$, $J'=3.5$ lines. Here the spin-orbit splitting is resolved so that P , Q , and R lines terminating on both upper-state $N=J+\frac{1}{2}$ and $N=J-\frac{1}{2}$ spin components are seen. (b) The $7d \Delta$, $v=0$ ($n^*=6.14$, 44090 cm^{-1})- $A^2\Pi_{3/2}$, $v''=0$, $J''=3.5$ lines. Here the spin-orbit splitting is not resolved and a four-line pattern is observed. The scans are linear in frequency and the lowest- and highest-frequency lines are labeled by their wave numbers.

level of the $A^2\Pi_{3/2}$ state. For $^2\Pi$ Rydberg states, transitions to the $N'=1, 2$, and 3 levels are observed while, for $^2\Delta$ Rydberg states, transitions are possible only to $N'=2$ and 3 levels.

As a first approximation, the Rydberg electron can be treated as if it moves in the field of a monopole at long range. The energies are then given by the familiar expression

$$E_{n^*} = I_P - R/(n^*)^2, \quad (1)$$

where I_P is the adiabatic ionization potential, R is the Rydberg constant, $n^* = n - \mu$, and μ is the quantum defect. The quantum defect parametrizes the complicated interactions that the Rydberg electron experiences inside the core and varies slowly with energy within a given nl series. Contributions to the long-range potential, mainly from the dipole moment, but also from the higher-order core multiple moments, will be evident in the quantum

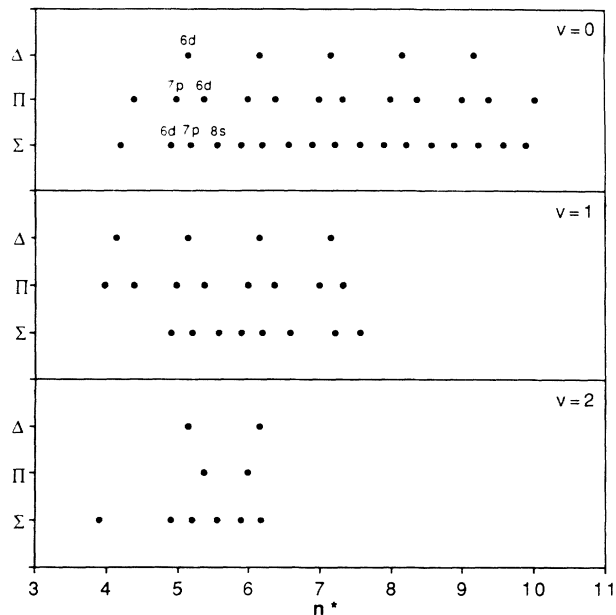


FIG. 2. n^* plot for all observed Rydberg states of CaF. All six series (s , p , $d \Sigma$, p , $d \Pi$, and $d \Delta$) are plotted together for the same vibrational quantum number. Note that the six series derived from the core-penetrating $l \leq 2$ orbitals form a series of supercomplexes rather than isolated l complexes. The nl labels are the nominal (i.e., dominant) l character of each member of the lowest-energy observed $v=0$ supercomplex ($4.8 < n^* < 5.7$). This is an example of the most extensive l mixing ever observed among all of the core-penetrating series. Although less complete, the $v=1$ and 2 series are almost perfect replicas of the $v=0$ series.

defect as well. The quantum defect is usually positive and its magnitude decreases rapidly with increasing l because the $l(l+1)/r^2$ centrifugal barrier prevents the Rydberg electron from penetrating into the core. If the states are represented as a function of n^* , where

$$n^* \equiv [R/(I_P - E_{n^*})]^{1/2}, \quad (2)$$

and the ionization potential is chosen correctly, n^* values of consecutive members of a Rydberg series will differ by approximately 1 because of the nearly constant quantum defect. We present n^* plots for the observed $v=0, 1$, and 2 levels in Fig. 2. The replicated patterns illustrated by Fig. 2 demonstrate the correctness of our assignments and the absence of any hint of isolated s , p , or d complexes. For $v=0$, six series are shown which converge to an ionization potential of $47005 \text{ cm}^{-1} \pm 20 \text{ cm}^{-1}$. There are one Δ , two Π , and three Σ series. These are the six series expected for an l -mixed supercomplex. Portions of similar series are shown converging to the $v=1$ ($47685 \pm 20 \text{ cm}^{-1}$) and $v=2$ ($48365 \pm 20 \text{ cm}^{-1}$) levels of the ion; thus, $\omega_e(\text{CaF}^+ X^1\Sigma^+) = 680 \pm 20 \text{ cm}^{-1}$. If these values of the $v=0, 1$, and 2 ionization potentials are varied by $\pm 20 \text{ cm}^{-1}$, the states can no longer be fitted into series. To our knowledge, the best previous determination of the CaF ionization potential is $44800 \pm 800 \text{ cm}^{-1}$, from the unpublished

electron-bombardment measurement of the CaF^+ appearance potential by Hildenbrand.¹⁰ The largest deviation from smooth n^* plots occurs for the $v=0$ Π state at $n^*=7.313$ which falls below where it would be expected by comparison with adjacent members of the series at $n^*=6.353$ and 8.343 . This large level-shift perturbation is undoubtedly related to the absence of the $n^*=6.35$, $v=1$ Π state that is expected to occur at about the same energy as the $n^*=7.313$, $v=0$ Π state. Such $\Delta v=1$, $\Delta l=0$, $\Delta \lambda=0$ perturbations provide a useful measure of the internuclear-distance dependence of the quantum-defect function $\mu_{\lambda}(r)$.¹¹

Ligand-field calculations have shown that the valence states of CaF can be represented as linear combinations of free Ca^+ -ion nl states.^{1,12,13} In particular, in the $\text{CaF } A^2\Pi$ state, the single occupied orbital outside the CaF^+ closed-shell core consists of 69% $4p$ and 24% $3d$ atomic Ca^+ character.¹ Therefore, the $\Delta l = \pm 1$ atomic selection rule predicts strong electronic dipole transitions from the $\text{CaF } A$ state to s and d Rydberg series, accompanied by ~ 2.9 times weaker transitions to p and f series. An initial assignment of the Rydberg states to n and l quantum numbers has been accomplished by extrapolating the quantum defects (modulo 1) of the observed Rydberg series to the previously assigned low Rydberg and valence states (see Fig. 3). This immediately determines the absolute integer value of the principal quantum number n and yields absolute quantum defects for all members of each series. As expected, Rydberg series of nominal (i.e., dominant) s , p , and d character are observed. However, unexpectedly we have detected no trace of an f series. The s , p , and d core-penetrating series are, like their valence-state precursors, of strongly l -mixed character.

One Δ Rydberg series ($\mu=0.87$) has been observed, but the two lowest members of this series have not yet been located. The series is assigned as $d \Delta$ because its quantum defect is too large to belong to the nonpenetrating f series. Predictions of the location of the lowest lying $3d \Delta$ state suggest that it is also associated with this series. The $3d \Delta$ state is predicted by Rice, Martin, and Field¹ to be at about 24950 cm^{-1} , corresponding to n^* of 2.23 ($\mu=0.77$). Another prediction, made by Törring, Ernst, and Kändler,¹² places the $3d \Delta$ state at about 17690 cm^{-1} ($\mu=1.065$). It is puzzling that the $f \Delta$ series does not appear in our OODR spectra. Perhaps the core dipole induces l mixing at long range in the nonpenetrating $l \geq 3$ series. The extremely small quantum defects of these $l \geq 3$ series ensure near perfect $l\lambda$, $(l+1)\lambda$ degeneracies (which makes irrelevant the approximate l^{-1} dependence of the dipole-core l -mixing matrix element). The expected $A^2\Pi \rightarrow nf(\Delta, \Pi, \Sigma^+)$ transitions might be unobservable because the $3d \rightarrow nf$ oscillator strength is diluted into many $l \geq 3$ series.

Both of the Π series extrapolate to previously observed low Rydberg and valence states. One of the Π series extrapolates to the E' and A states with only a small deviation

in the quantum defect. We have assigned this as a $p \Pi$ series ($\mu=2.02$) based on the ligand-field calculations.¹ The other Π series extrapolates to the F and C states, but with a much larger decrease in the quantum defect for the C state. This series is assigned as $d \Pi$ ($\mu=0.65$). The anomalously small quantum defect of the C state is probably due to the reverse polarization of the nominally $3d \Pi$ orbital towards the ligand (due to M -centered, ligand-induced mixing of $3d$ with $4p$).^{1,14} Preliminary indications of the spin-orbit constants in the Π series support these extrapolations as well as the nominal l assignments. The spin-orbit constants of the $(n+1)p \Pi$ states ($n^*=4.98, 5.98$, etc.) are about twice as large as those of the slightly higher-lying $nd \Pi$ states ($n^*=5.35, 6.35$, etc.). This $\sim 2:1$ ratio is also observed in the A and C states where the spin-orbit constants are 71 and 29 cm^{-1} , respectively.¹

Two of the Σ series extrapolate to low Rydberg and valence states with only small deviations in the quantum defect, while the third extrapolates to the reverse-polarized C' state with a large decrease in the quantum defect. One Σ series extrapolates to the X state and is assigned as nominally $s \Sigma$ ($\mu=2.45$). This assignment is supported by preliminary fits of the spin-rotation constants in this series which are on the order of 10^{-3} cm^{-1} , similar to that of the X state. The spin-rotation splittings within a CaF Rydberg Σ series should remain almost independent of n^* . The spin-rotation splitting is a second-order effect involving the product of the spin-orbit operator, which scales as $(n^*)^{-3}$, and the $BJ \cdot L$ operator which is independent of n^* . Since the energy denominator between interacting Σ and Π states (at a particular J value) also scales as $(n^*)^{-3}$, the spin-rotation splitting should be independent of n^* . The series which extrapolates to the B state (42%, $3d$, 38% $4p$)¹ is assigned as nominally $d \Sigma$ ($\mu=1.10$) and the remaining Σ series (which extrapolates to the C' state) is assigned as nominally $p \Sigma$ ($\mu=1.83$). The spin-rotation constants in these series are also consistent with those of their valence precursor states. The large quantum-defect deviation for the lowest member of the $p \Sigma$ series may also be due to a reverse-polarization effect similar to that observed for the lowest member of the $d \Pi$ series. As inexplicable as the absence of an $f \Delta$ series, there is no trace of either an $f \Pi$ or an $f \Sigma$ series.

We are currently recording higher- J spectra in order to measure the Λ -doubling constants of the observed Π states and more accurate spin-rotation constants of nearby Σ states. Deperturbation will provide information on the extent of l mixing as well as improved molecular constants. A multichannel quantum-defect analysis¹¹ should make it possible to separate the contributions to the l mixing and quantum defects due to short-range interactions (e.g., ligand field) from those produced by long-range interactions^{5,7} (including the ion-core dipole moment). Measuring the dipole moment of the ion core will be simplified if nonpenetrating f and higher l states

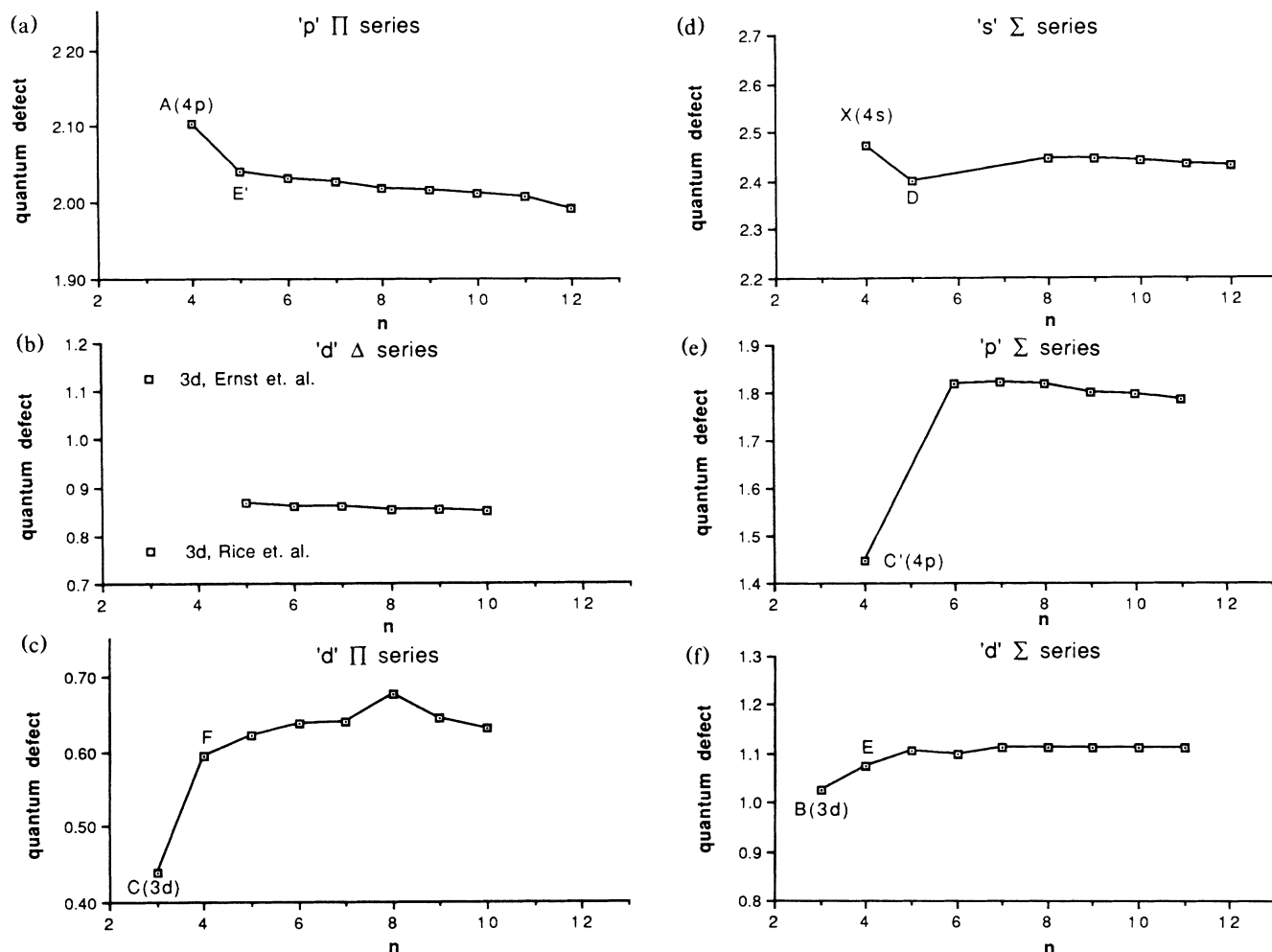


FIG. 3. Absolute quantum defects plotted vs integer n values. Previously observed valence and Rydberg states are labeled on segments (a), (c), (d), (e), and (f). Two predicted (Refs. 1 and 12) locations of the not yet observed $3d \Delta$ state are shown in segment (b).

can be observed, because the l mixing would then be due solely to the long-range interaction of the Rydberg electron with the multipolar ion core.⁷ It is hoped that OODR spectra via the $C^2\Pi$ state will reveal the elusive $nf \Delta, \Pi,$ and Σ states owing to the dominant $3d$ character of the C state.

We thank Ernest J. Hill for the use of his spectrum plotting program. A.J.M. thanks the Canada Council for the award of a Killam Research Fellowship. This research is supported by the National Science Foundation under Grant No. PHY87-09759.

^(a)Present address: Inc-11, c345, Los Alamos National Laboratory, Los Alamos, NM 87545.

^(b)Permanent address: Department of Chemistry, University of British Columbia, 2036 Main Mall, Vancouver, British Columbia, Canada V6T 1Y6.

¹S. Rice, H. Martin, and R. Field, *J. Chem. Phys.* **82**, 5023 (1985).

²R. S. Mulliken, *J. Am. Chem. Soc.* **86**, 3183 (1964).

³G. Herzberg, *Annu. Rev. Phys. Chem.* **38**, 27 (1987).

⁴L. C. O'Brien, C. R. Brazier, S. Kinsey-Nielsen, and P. F. Bernath, *J. Phys. Chem.* **94**, 3543 (1990), and references therein.

⁵Ch. Jungen and E. Miescher, *Can. J. Phys.* **47**, 1769 (1969).

⁶G. Herzberg and Ch. Jungen, *J. Chem. Phys.* **77**, 5876 (1982).

⁷E. E. Eyler and F. M. Pipkin, *Phys. Rev. A* **27**, 2462 (1983).

⁸G. Herzberg and Ch. Jungen, *J. Chem. Phys.* **84**, 1181 (1986).

⁹S. Fredin, D. Gauyacq, M. Horani, Ch. Jungen, G. Lefevre, and F. Masnou-Seeuws, *Mol. Phys.* **60**, 825 (1987), and references therein.

¹⁰D. Hildenbrand (private communication).

¹¹G. Herzberg and Ch. Jungen, *J. Mol. Spectrosc.* **41**, 425 (1972).

¹²T. Törring, W. E. Ernst, and J. Kändler, *J. Chem. Phys.* **90**, 4927 (1989).

¹³S. L. Davis, *J. Chem. Phys.* **89**, 1656 (1988).

¹⁴W. E. Ernst and J. Kändler, *Phys. Rev. A* **39**, 1575 (1989).